

Microfabrication of Concave Micromirror for Microbial Cell Trapping Using Köhler Illumination by XeF₂ Vapor Etching

Akihiro Matsutani,^{1*} Mina Sato,¹ Koichi Hasebe,¹ and Ayako Takada²

¹Semiconductor and MEMS Processing Division, Technical Department, Tokyo Institute of Technology,
4259 Nagatsuta, Yokohama 226-8503, Japan

²Biomaterials Analysis Division, Technical Department, Tokyo Institute of Technology,
4259 Nagatsuta, Yokohama 226-8501, Japan

(Received December 11, 2018; accepted March 29, 2019)

Keywords: single-cell isolation, concave micromirror, XeF₂, etching, Si, cell trapping

We demonstrated a Si-based concave micromirror array for cell trapping that was fabricated by XeF₂ vapor etching. We also examined the optical properties of the focal image of each concave micromirror. In addition, yeast cell trapping was realized at the focal point of a concave micromirror of approximately 35 μm diameter by Köhler illumination using a halogen lamp. The proposed process is useful for the microfabrication of various Si-based microstructure devices, such as microchannels and micro-electromechanical systems (MEMS).

1. Introduction

Single-cell isolation is regarded as an important elemental technique in cell analysis, because cells show considerable heterogeneity, even in the same colony. However, conventional biochemical techniques, i.e., bulk analyses, can provide only average values obtained from large numbers of cells. Research on the behavior of an individual cell will become possible by using single-cell isolation techniques, leading to new developments in research on drug discovery and cell engineering. To realize single-cell isolation, we have developed a microenclosure with a micropillar array structure and succeeded in the single-cell isolation and size separation of *Escherichia coli* and yeast cells.^(1,2) On the other hand, single-cell manipulation is also regarded as an important elemental technique in cell analysis. Optical tweezers using laser light are widely employed for the manipulation of microbial cells.^(3–6) The principle of a single-beam gradient force trap is, in essence, optical levitation by radiation pressure.⁽⁷⁾ In a typical measurement system, laser light is focused by a microscope objective lens, and cells and particles can be trapped at its focal point. In this case, the focused spot is a single point. We aim to develop a two-dimensional array for the single-cell manipulation of microorganisms by fusing single-cell isolation techniques. We believe that if an optical trap with a concave micromirror, as shown in Fig. 1, can also be added to the above single-cell isolation structure, the range of applications of our cell isolation chip will expand. Our concept is cell trapping using a two-dimensional concave micromirror array under Köhler illumination. Köhler

*Corresponding author: e-mail: matsutani.a.aa@m.titech.ac.jp
<https://doi.org/10.18494/SAM.2019.2235>

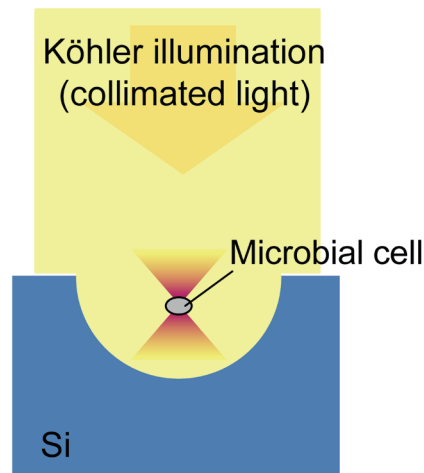


Fig. 1. (Color online) Schematic diagram of cell trapping at focal point of Si-based concave micromirror.

illumination is a method of illumination with parallel (collimated) light at a sample position. If a concave micromirror is placed under light provided by this illumination method, the light is focused at its focal point. Note that various methods have been reported for the fabrication of concave micromirrors.^(8–13) Merenda *et al.*⁽⁸⁾ reported multiple optical tweezers with a miniaturized high-numerical-aperture (NA) focusing mirror. However, they used commercially fused silica microlens arrays as replica molds. On the other hand, if concave micromirrors can be fabricated by researchers themselves, the diameter and array pitch of a concave micromirror can be optimized according to the research purpose. For this purpose, it is desirable to use a Si-based micro-electromechanical system (MEMS) fabrication process. Generally, wet etching is used for the microfabrication of an isotropic etching profile. However, it is difficult to fabricate an isotropic concave profile through a small opening mask by wet etching owing to the surface tension. The etching profile of vapor etching is isotropic owing to the chemical reaction between the etching gas and the material surface. Vapor etching using XeF_2 is widely employed for Si etching.^(14–16) Thus, we introduced XeF_2 gas-phase etching for the fabrication of a Si-based concave micromirror.

In this paper, we report the microfabrication of a concave micromirror by XeF_2 vapor etching and the optical properties of the focal image of the fabricated micromirror. We also report the trapping of microbial cells using Köhler illumination and the concave micromirror.

2. Microfabrication of Si-based Concave Micromirrors

Figure 2 shows a schematic diagram of the XeF_2 vapor etching system used in our experiment. We used a stainless-steel chamber to avoid chemical reactions between the chamber wall material and the etching species. A borosilicate glass was used as a viewing window. First, a small aperture pattern was formed by direct drawing using electron beam (EB) lithography or by a conventional photolithography technique. Next, the Si substrate

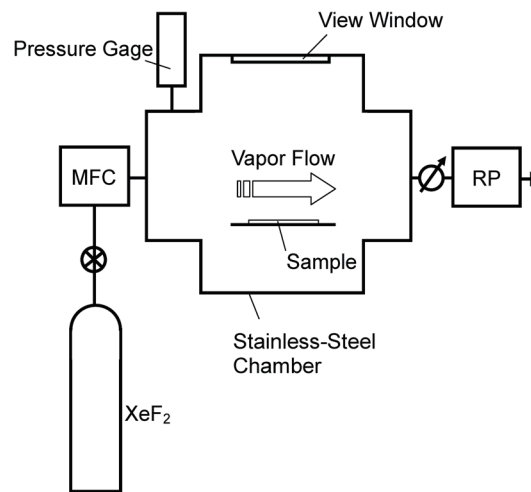


Fig. 2. Etching system using XeF_2 vapor in this experiment.

was etched isotropically by supplying XeF_2 vapor from the submicron opening of the etching mask. Finally, the Si substrate was etched isotropically by supplying XeF_2 vapor from the small opening of the etching mask.

Sugano and Tabata reported the effects of aperture size and pressure on the XeF_2 etching of silicon.⁽¹⁷⁾ However, in their report, the size of the opening ranged from 10 to 175 μm . For the fabrication of a concave micromirror, a fabrication process with a smaller aperture size is necessary. We investigated the relationship between the etching distance and the aperture size with aperture sizes of 20–500 nm. In this experiment, since the etching method was pure chemical etching, an isotropic etching profile with a hemispherical shape was expected. Figure 3(a) shows the etching depth and lateral distance of Si as a function of the opening width for an etching time of 4 min. When the aperture width was 20 nm, the etching width was 1190 nm, which is approximately twice the etching depth (590 nm). These values correspond to a hemispherical etching profile. On the other hand, when the aperture width was 500 nm, the etching width was 6810 nm, which is about 1.7 times the etching depth (4070 nm). In other words, the etching profile was not hemispherical but elliptical. The larger the opening width, the greater the etching width, which was smaller than twice the etching depth. Figure 3(b) shows the ratio of the opening width to the net etching width. This ratio was 1–1.3. In other words, the etching profile was isotropic. It is understood that the mechanism of the XeF_2 vapor etching process used in this experiment is dominated by chemical etching. In the process chamber and near the sample, XeF_2 , Xe, and F derived from the supply gas and SiF_4 as a reaction product are included. Since the etching pressure is 200 Pa, the mean free path is estimated to be about 30 μm in terms of N_2 molecules. Therefore, the gas is deduced to be sufficiently replaced even in the etched concave space. Figure 3(c) shows a cross-sectional scanning electron microscopy (SEM) image of a concave profile with various opening widths obtained by XeF_2 vapor etching for 2 min. It was found that the curvature radius or profile can be controlled by varying the opening width.

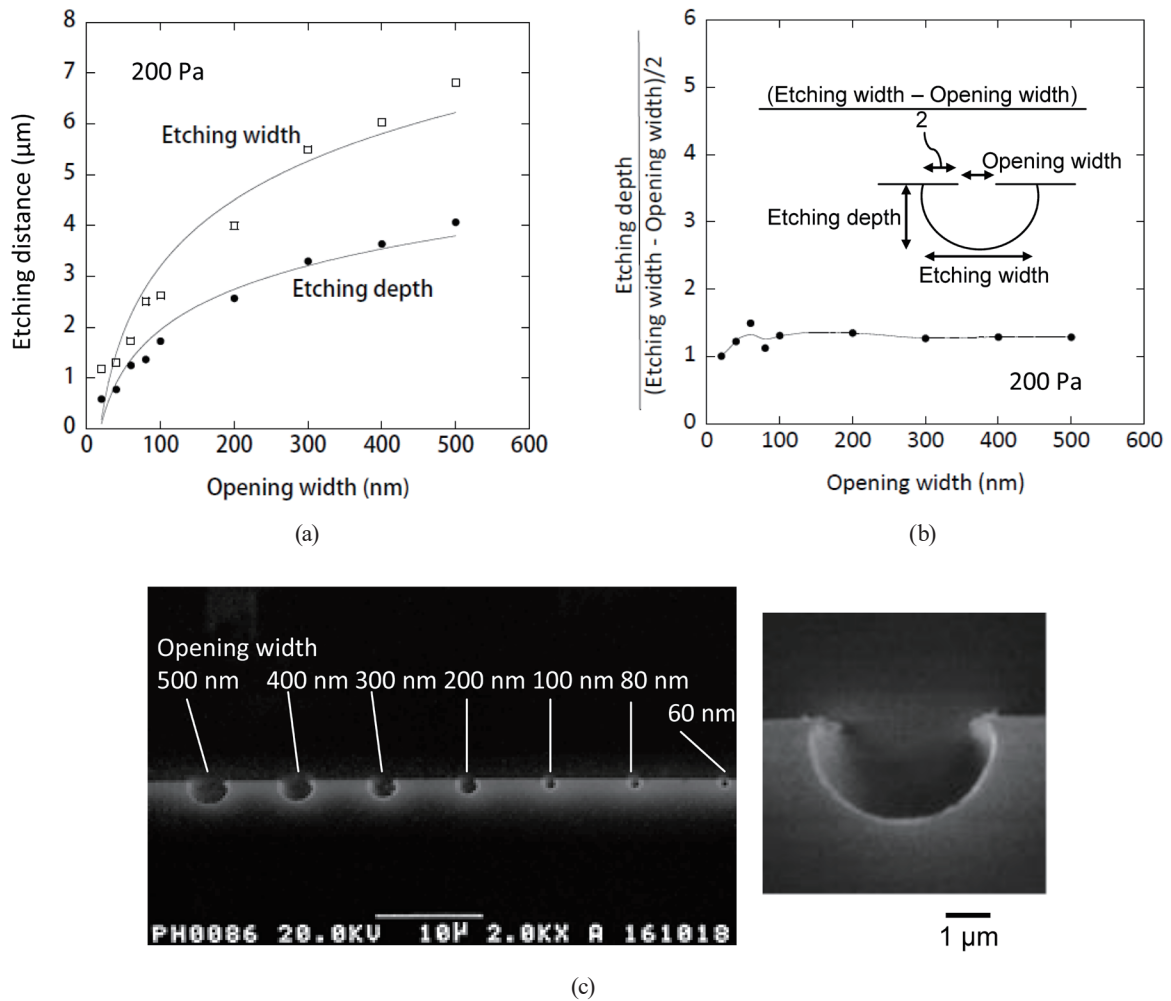


Fig. 3. (a) Etching depth and lateral distance of Si as a function of the opening width and (b) ratio of the opening width to the net etching width. (c) Cross-sectional SEM image of a concave profile with various opening widths obtained by XeF_2 vapor etching.

3. Optical Characteristics of Concave Micromirror

We fabricated a concave micromirror array. The initial opening diameter of the etching mask was $5 \mu\text{m}$. The etching pressure was about 120 Pa and the etching time was 25 min. First, we confirmed that the curved surface of the fabricated concave micromirrors reflects light. Figure 4(a) shows an optical microscopy image of concave micromirrors illuminated by the following method.⁽¹⁸⁾ Light from a halogen lamp light source was irradiated on the concave micromirrors using two quartz fibers. This corresponds to dark-field illumination. Under this illumination, we observed the concave micromirrors using an optical microscope (Meiji Techno, ML 7100) and a $10\times$ objective lens (Olympus MD Plan 10, NA: 0.25). From this figure, it was found that the curved surface of the fabricated concave micromirrors reflects light. Figure 4(b) shows an optical microscopy image of the concave micromirror array observed under Köhler

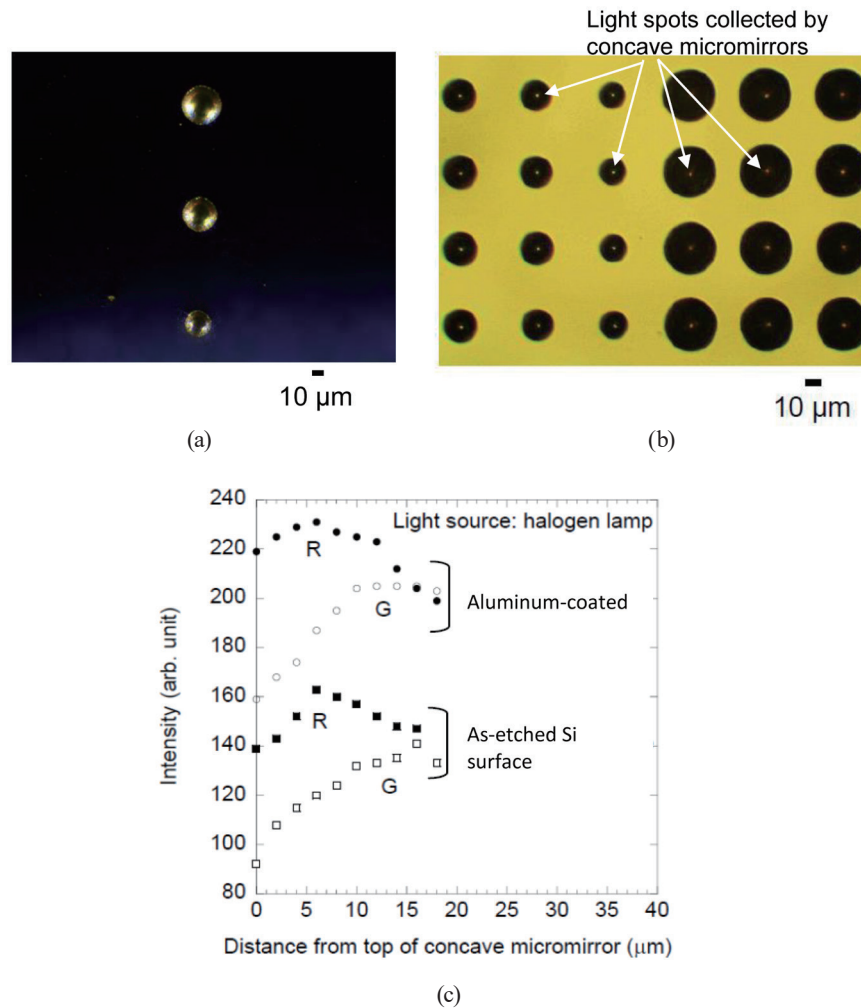


Fig. 4. (Color online) (a) Top-view optical microscopy image of concave micromirrors under dark-field illumination,⁽¹⁸⁾ (b) top-view image of concave micromirror array observed under Köhler illumination using halogen lamp, and (c) intensity distributions along the optical axis for the as-etched and aluminum-coated concave micromirror surfaces.

illumination using the halogen lamp. From this image, it can be seen that the reflected light by Köhler illumination is collected at the focal point of each concave micromirror. Figure 4(c) shows the intensity distributions along the optical axis for the as-etched concave micromirror surface and the concave micromirror surface coated with an aluminum film of 100 nm thickness. This concave micromirror was illuminated with a parallel white light source (halogen lamp). The concave micromirror had a diameter of about $35 \mu\text{m}$ and its bottom surface was approximately $17 \mu\text{m}$ from the substrate surface. It can be seen that the intensity of light was increased by coating the micromirror with the aluminum thin film. In addition, the position of maximum intensity (focal point) differs between red (R) light and green (G) light. Here, R light and G light represent the respective components of R and G in the RGB color image of a mirrorless interchangeable lens camera (Nikon1J1) in Fig. 4(b). In the measurement of intensity position, the stage of the microscope was moved up and down while monitoring with a

noncontact distance sensor (Keyence, EX-V05) using eddy current. The images of the concave micromirror every movement of $2\ \mu\text{m}$ were recorded with a camera. The intensities of the R and G images extracted from these RGB images were measured. Since there is no chromatic aberration in imaging with a reflecting mirror, the focal positions of R light and G light should be the same. We deduced that this is due to the chromatic aberration of the lenses of the illumination and imaging systems. In addition, the position of maximum intensity for R light was $6\ \mu\text{m}$ from the substrate surface. This value corresponds to a distance of about $11\ \mu\text{m}$ from the bottom surface of the concave micromirror. The midpoint between the points of maximum intensity for R light and G light was about $8\ \mu\text{m}$ from the substrate surface. The focal length of the spherical micromirror is half the radius. Therefore, this concave micromirror was estimated to be almost spherical in the wavelength range of the halogen light source.

Figures 5(a) and 5(b) respectively show the optical microscopy image and intensity profile of the focal spot of a concave micromirror illuminated with red laser light ($650\ \text{nm}$). The diameter

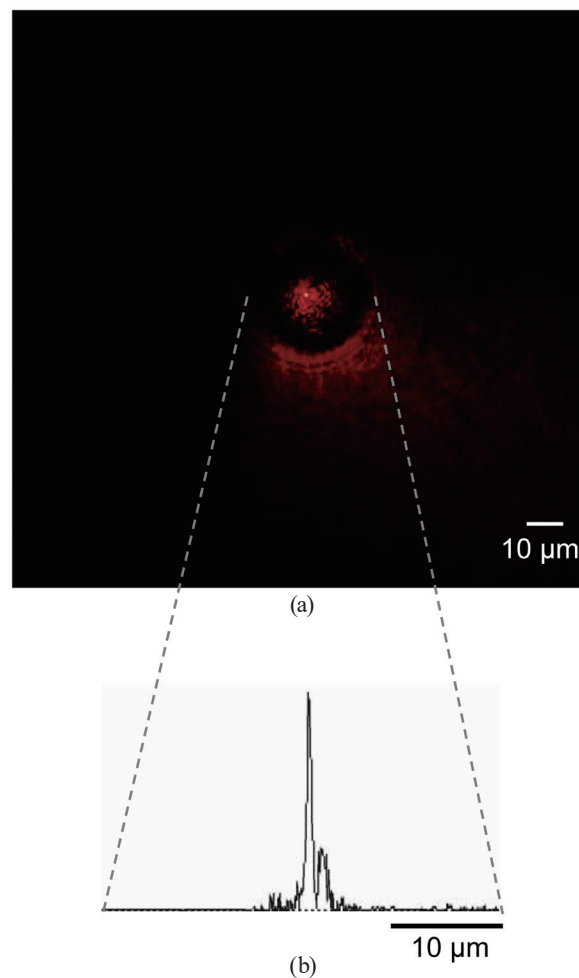


Fig. 5. (Color online) (a) Top-view optical microscopy image and (b) intensity profile of focal spot of the concave micromirror illuminated with red laser light.

of this concave micromirror was 35 μm . This micromirror shows that the incident light was focused to a beam spot of about 1 μm . However, the focused light exhibited scattering near the center, which was due to the surface roughness of the concave micromirror. This surface roughness was caused by a reaction derived from the chemical etching of Si. In the XeF_2 vapor etching of Si, the formation of SiF_2 and SiF_3 complexes is a nonactivated process. Therefore, their formation is not surface-site-dependent. Si atoms are removed from random sites on the surface, and the surface roughness increases during etching with XeF_2 exposure.⁽¹⁹⁾ This roughness can be reduced to about 5 nm.⁽²⁰⁾ Therefore, it is considered that light focusing with a higher signal-to-noise (S/N) ratio can be realized by optimizing the etching conditions.

4. Trapping Yeast Cells with Köhler Illumination and Concave Micromirrors

First, we confirmed the bottom surface and focal position of the fabricated concave micromirrors. Figures 6(a) and 6(b) show photographs of the focal position and bottom surface of concave micromirrors under Köhler illumination, respectively. Figure 6(c) shows a cross-sectional SEM image of the concave micromirror used in this experiment. When focusing on the bottom surface of the concave micromirrors, the surface was out of focus and blurred. In other words, by adjusting the microscope at the focal position, cells trapped at the focal point can be clearly observed. It can be determined whether cells are trapped at the focal position using this observation method. We used a 30 W halogen lamp as a light source for Köhler illumination. The diameter of the condenser lens in the lamp house was 15 mm. A Si substrate with a concave micromirror array was placed at the center of a square polystyrene container ($30 \times 30 \text{ mm}^2$) and fixed with double-sided tape. Next, a yeast cell suspension was poured into the container to a depth of about 2 mm. The size of the yeast cells used in this experiment was approximately 5 μm and the density of yeast cells in the suspension was 4×10^6 cells/ml. In this experiment, concave micromirrors with a diameter of 35 μm were used. The power collected by a concave micromirror with a diameter of 35 μm was estimated to be about 0.08 mW. Tachibana and Ukita have reported that the minimum trapping power taking into account gravity and the buoyancy and thermal motion of polystyrene particles with a diameter of 5 μm is about 0.02 mW.⁽²¹⁾ The density of polystyrene is slightly higher than 1 g/cm^3 . The density of yeast cells was also estimated to be similar to or on the same order as that of polystyrene. Therefore, we believe that it is possible to trap yeast cells using the observation system employed in this experiment. Figures 6(d)–6(g) show the trapping of yeast cells using Köhler illumination and concave micromirrors. In this experiment, there was a gentle flow from left to right. As shown in these figures, a yeast cell flowing from the left was trapped at the focal position of a concave micromirror. Yeast cells captured at the focal point of the concave micromirror oscillated at the focal point and its neighborhood. We consider that the yeast cell was constrained by approximately the minimum trapping power. Figure 6(h) shows the movement trajectory of two yeast cells. The trajectory of a trapped yeast cell is shown by the blue line and that of a yeast cell that did not reach the concave micromirror is shown by the red line. After forcefully vibrating the sample stage of the microscope in the left and right directions, no trapped yeast cells were observed at the focal point or the bottom surface. Assuming that yeast cells are

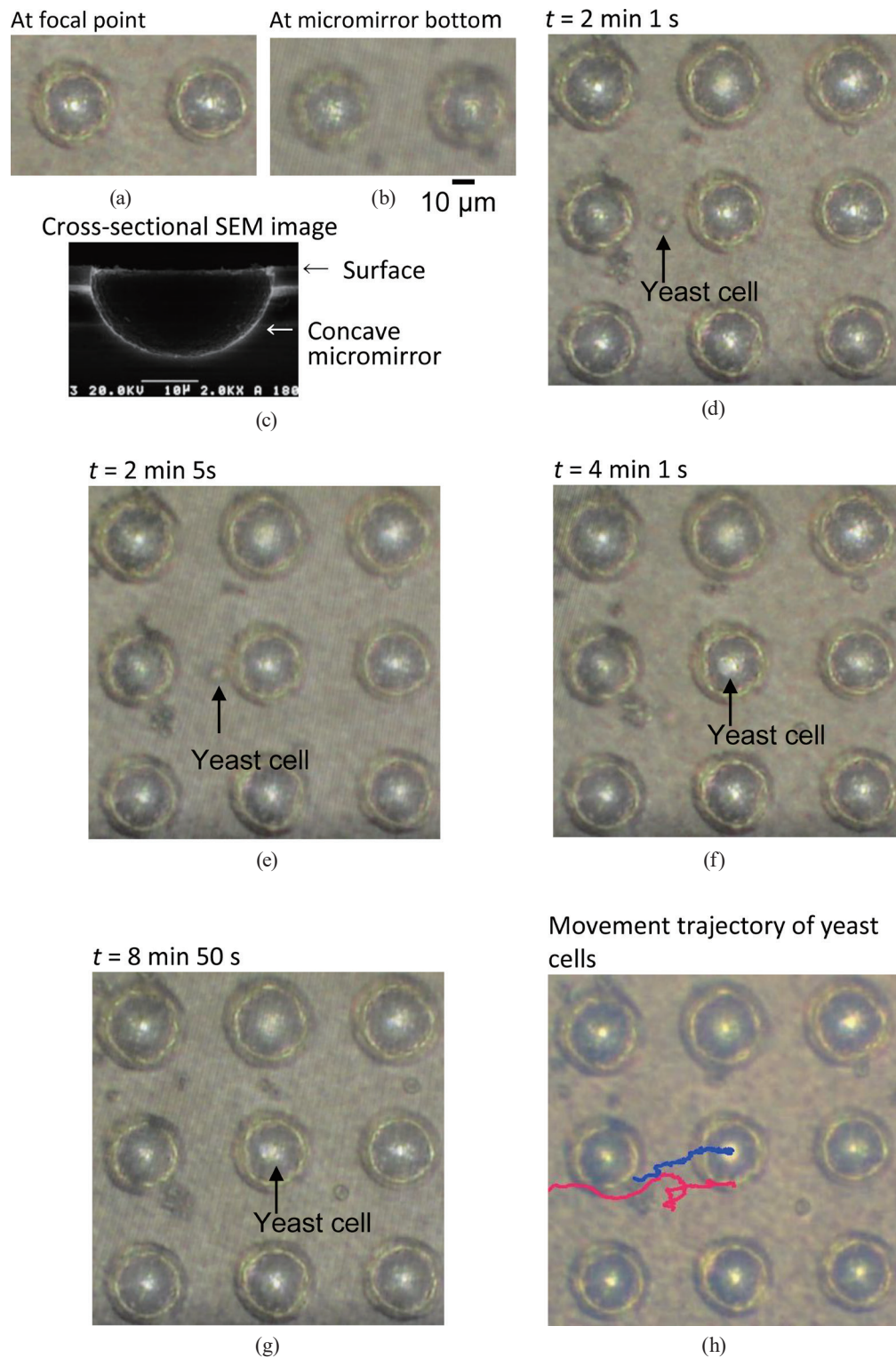


Fig. 6. (Color online) Top-view images of concave micromirrors used in optical microscopy: (a) focal point, (b) bottom surface of concave micromirrors, (c) magnified cross-sectional SEM image of the etched concave profile, (d)–(g) trapping of yeast cells using Köhler illumination and concave micromirrors, and (h) movement trajectory of yeast cells.

hard spheres, the resistance force in viscous fluid is expressed as $6\pi\eta Ru$ according to Stokes's law. Here, η is the viscosity, R is the radius of the particle, and u is the flow velocity. When η is ~ 1 mPa·s, R is 1.5–2.5 μm , and when u is 1–5 $\mu\text{m/s}$, the resistance force can be estimated as 30–230 fN. In this experiment, since the yeast cell was captured in the fluid flow, the capture force can be estimated at least on the order of the above mentioned value. From these results, we believe that the trapping of yeast cells was realized using Köhler illumination and a concave micromirror.

5. Conclusions

We demonstrated the use of XeF₂ vapor etching to fabricate a concave micromirror array and examined the optical properties of the focal image of each concave micromirror. In addition, we realized the trapping of yeast cells using Köhler illumination and a concave micromirror. We consider that if an optical trap with a concave micromirror can also be added to the microenclosure array for single-cell isolation, then the range of applications of our cell isolation chip will expand. We believe that the proposed method will be useful for multiple cell manipulation techniques with improved light collection efficiency.

Acknowledgments

This work was supported by JSPS KAKENHI Grant Number JP17K05020.

References

- 1 A. Matsutani and A. Takada: *Jpn. J. Appl. Phys.* **49** (2010) 127201.
- 2 A. Matsutani and A. Takada: *Jpn. J. Appl. Phys.* **51** (2012) 087001.
- 3 A. Ashkin, J. M. Dziedzic, J. E. Bjorkholm, and S. Chu: *Opt. Lett.* **11** (1986) 288.
- 4 H. Liang, W. H. Wright, S. Cheng, W. He, and M. W. Berns: *Exp. Cell Res.* **204** (1993) 110.
- 5 A. Ashkin: *Proc. Natl. Acad. Sci. U.S.A.* **94** (1997) 4853.
- 6 H. Zhang and K. K. Liu: *J. R. Soc. Interface* **5** (2008) 671.
- 7 A. Ashkin and J. M. Dziedzic: *Appl. Phys. Lett.* **19** (1971) 283.
- 8 F. Merenda, J. Rohner, J. M. Fournier, and R. P. Salathé: *Opt. Express* **15** (2007) 6075.
- 9 Y. S. Ow, M. B. H. Breese, and S. Azimi: *Opt. Express* **18** (2010) 14511.
- 10 G. Q. Cui, J. M. Hannigan, R. Loeckenhoff, F. M. Matinaga, M. G. Raymer, S. Bhongate, M. Holland, S. Mosor, S. Chatterjee, H. M. Gibbs, and G. Khitrova: *Opt. Express* **14** (2006) 2289.
- 11 F. M. Matinaga, A. Karlsson, S. Machida, Y. Yamamoto, T. Suzuki, Y. Kadota, and M. Ikeda: *Appl. Phys. Lett.* **62** (1993) 443.
- 12 D. C. Appleyard and M. J. Lang: *Lab Chip* **7** (2007) 1837.
- 13 J. Albero, L. Nieradko, C. Gorecki, H. Ottevaere, V. Gomez, H. Thienpont, J. Pietarinen, B. Päivänranta, and N. Passilly: *Opt. Express* **17** (2009) 6238.
- 14 H. F. Winters and J. W. Coburn: *Appl. Phys. Lett.* **34** (1979) 70.
- 15 J. S. Park, H. D. Park, and S. G. Kang: *Sens. Actuators, A* **117** (2005) 1.
- 16 C. Easter and C. B. O'Neal: *J. Microelectromech. Sys.* **18** (2009) 1054.
- 17 K. Sugano and O. Tabata: *Microsyst. Technol.* **9** (2002) 11.
- 18 A. Matsutani: *OYO BUTURI* **87** (2018) 885 (in Japanese).
- 19 V. S. Aliev and V. N. Kruchinin: *Surf. Sci.* **442** (1999) 206.
- 20 K. Sugano and O. Tabata: *J. Micromech. Microeng.* **12** (2002) 911.
- 21 S. Tachibana and H. Ukita: *Kogaku* **27** (1998) 524 (in Japanese).

Appendix: Control of concave profile of micromirror by two-step etching

We propose a two-step etching process using XeF_2 vapor etching to control the concave profile for the fabrication of micromirror arrays. The concave micromirror preferably has a parabolic profile from the viewpoint of correction of the aberration to obtain a good focusing spot. We conducted a two-step etching process to control the concave profile. The principle of this process is shown in Fig. A1. The first step of etching involves Cl_2 -based inductively coupled plasma (ICP) etching, where the etching depth is on the 100 nm order (300 nm in this experiment); the second step is conducted by XeF_2 vapor etching, where the etching depth is on the μm order. In the initial Cl_2 -ICP etching, the etching profile is vertical. In the second step using XeF_2 vapor, the etching profile is isotropic since the XeF_2 vapor etching involves only chemical etching. Figures A2(a) and A2(b) show etching profiles obtained by conventional XeF_2 vapor etching and the proposed two-step etching, respectively. The etching profile became parabolic during the two-step process. In the future, a wide range of concave profiles may be realized by optimizing the conditions of the two-step etching process for the fabrication of concave micromirrors.

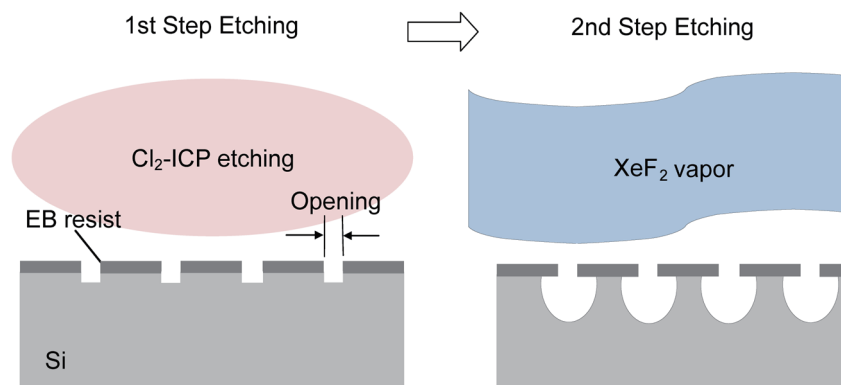


Fig. A1. (Color online) Principle of the two-step etching for controlling the concave profile.

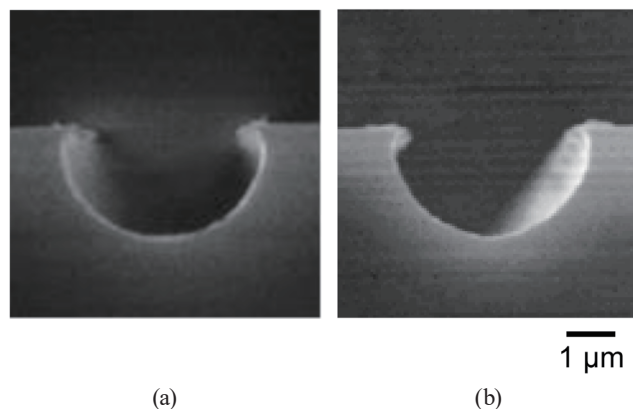


Fig. A2. Etching profiles obtained by (a) conventional XeF_2 vapor etching and (b) the proposed two-step etching.